RPC observation of the development and evolution of plasma interaction boundaries at 67P/Churyumov-Gerasimenko

K. E. Mandt, A. Eriksson, N. J. T. Edberg, C. Koenders, T. Broiles, S. A. Fuselier, C. Goetz, Pierre Henri, Z. Nemeth, M. Alho, et al.

Monthly Notices
of the
ROYAL ASTRONOMICAL SOCIETY

MNRAS **462,** S9–S22 (2016)
Advance Access publication 2016 July 20

doi:10.1093/mnras/stw1736

RPC observation of the development and evolution of plasma interaction boundaries at 67P/Churyumov-Gerasimenko

K. E. Mandt,[1,2★] A. Eriksson,[3] N. J. T. Edberg,[3] C. Koenders,[4] T. Broiles,[1★] S. A. Fuselier,[1,2★] P. Henri,[5] Z. Nemeth,[6] M. Alho,[7] N. Biver,[8] A. Beth,[9] J. Burch,[1] C. Carr,[9] K. Chae,[1] A. J. Coates,[10] E. Cupido,[9] M. Galand,[9] K.-H. Glassmeier,[4] C. Goetz,[4] R. Goldstein,[1] K. C. Hansen,[11] J. Haiducek,[11] E. Kallio,[7] J.-P. Lebreton,[5] A. Luspay-Kuti,[1] P. Mokashi,[1] H. Nilsson,[12] A. Opitz,[6] I. Richter,[4] M. Samara,[13] K. Szego,[6] C.-Y. Tzou,[14] M. Volwerk,[15] C. Simon Wedlund[16] and G. Stenberg Wieser[12]

Affiliations are listed at the end of the paper

Accepted 2016 July 14. Received 2016 July 13; in original form 2016 May 19

ABSTRACT

One of the primary objectives of the Rosetta Plasma Consortium, a suite of five plasma instruments on-board the Rosetta spacecraft, is to observe the formation and evolution of plasma interaction regions at the comet 67P/Churyumov-Gerasimenko (67P/CG). Observations made between 2015 April and 2016 February show that solar wind–cometary plasma interaction boundaries and regions formed around 2015 mid-April and lasted through early 2016 January. At least two regions were observed, separated by an ion-neutral collisionopause boundary. The inner region was located on the nucleus side of the boundary and was characterized by low-energy water-group ions, reduced magnetic field pileup and enhanced electron densities. The outer region was located outside of the boundary and was characterized by reduced electron densities, water-group ions that are accelerated to energies above 100 eV and enhanced magnetic field pileup compared to the inner region. The boundary discussed here is outside of the diamagnetic cavity and shows characteristics similar to observations made on-board the Giotto spacecraft in the ion pileup region at 1P/Halley. We find that the boundary is likely to be related to ion-neutral collisions and that its location is influenced by variability in the neutral density and the solar wind dynamic pressure.

Key words: plasmas – solar wind – comets: general.

1 INTRODUCTION

The interaction of the solar wind with comets is unique compared to the interaction of the solar wind with unmagnetized planetary atmospheres. The high neutral outgassing rate of comets causes the interaction to begin at great distances from the comet itself through the process of mass loading of the solar wind (e.g. Biermann, Brosowski & Schmidt 1967; Galeev 1988; Johnstone 1995; Szegö et al. 2000). Spacecraft flybys of comets have observed several permanent and transient features of this interaction. These features remain poorly understood owing to a limited number of *in situ* observations and limitations of theoretical modelling imposed by computation time constraints. A further complication is caused by the fact that the plasma interaction structures are expected to be highly variable with time because they result from two opposite flows, both of which are highly unsteady with time (Gringauz & Verigin 1991).

Prior to Rosetta, all observations of comet-solar wind interaction were made using spacecraft flybys at high velocity (tens of km s^{-1}) through comets experiencing high outgassing rates, with the exception of the Giotto flyby of 26P/Grigg-Skjellerup (26P/GS), which had a relatively weak outgassing rate. The Rosetta mission (Glassmeier et al. 2007a) was launched in 2004 March and arrived at comet 67P/Churyumov-Gerasimenko (67P/CG) in 2014 August. Rosetta is unique compared to previous comet missions in several ways. First, Rosetta provides an opportunity to escort a comet from distances greater than 3.0 astronomical units (au), through perihelion at ∼1.3 au, and back out to distances greater than 3.0 au. Secondly, the outgassing rate of 67P/CG is low compared to comets from previous spacecraft flybys, making it more comparable to the

★ E-mail: kmandt@swri.org (KEM); tbroiles@swri.org (TB); sfuselier@swri.org (SAF)

Table 1. Comparison of flyby conditions for three spacecraft flybys of comet Halley, the Giotto flyby of 26P/Grigg-Skjellerup (26P/GS) and the Rosetta escort of 67P/CG. The ion pileup region, which is the focus of this study, is located between the ion velocity drop and the ion pileup boundary.

	Vega-1	Vega-2	Giotto		Rosetta (excursion)
Comet	1P/Halley	1P/Halley	1P/Halley	26P/GS	67P/CG
Date of observation	3/6/86	3/9/86	3/14/86	7/10/92	2015 Sept. 22–Oct. 11
Production rate (s^{-1})	1.5×10^{30}	5×10^{29}	3.8×10^{29}	7×10^{27}	$\sim 1 \times 10^{28}$
Distance from Sun (au)	0.792	0.834	0.903	1.01	1.4
Solar wind velocity (km s^{-1})	510	620	350–400	360	Variable
Closest approach (km)	8890	8030	605	200	Distance 300–1500
Spacecraft velocity (km s^{-1})	79.2	76.8	68.4	13.99	<2 m s^{-1}
Bow shock (km)	$5.5–10.0 \times 10^5$ (a)		5.98×10^5 (b)	1.67×10^4 (c)	Not observed
Bow shock along Sun–comet line (km)	2.70×10^5 (a)		3.9×10^5 (d)	1.7×10^4 (e)	
Mystery boundary (km)	n/a	n/a	5.50×10^5 (f)	1.05×10^4 (e)	
Cometopause (km)	1.73×10^5	1.6×10^5 (g)	1.4×10^5 (f)	1.8×10^3 (h)	
Cometopause along Sun–comet line (km)	n/a	n/a	5.0×10^4 (i)	n/a	
Ion velocity drop (km)			2.7×10^4 (j)		500–700 (k)
Ion pile up boundary (km)	1.1×10^4 (l)		1.0×10^4 (j)	n/a	Not observed
Contact surface (km)	n/a	n/a	4.6×10^3 (b,m)	n/a	$\sim$170 (n)

Notes. (a) Galeev et al. (1986); (b) Coates (2009); (c) Coates, Johnstone & Neubauer (1996); (d) Neubauer et al. (1986); (e) Neubauer et al. (1993); (f) Rème et al. (1988); (g) Gringauz & Verigin (1991); (h) Johnstone et al. (1993); (i) Gringauz et al. (1986a); Galeev (1988); (j) Schwenn et al. (1988); (k) 2015 April–November, this work; (l) Pätzold et al. (1997); (m) Neubauer (1988); (n) not observed during the excursion, but observed in 2015 July as reported by Goetz et al. (2016).

Giotto flyby of 26P/GS than the multiple spacecraft flybys of comet 1P/Halley (hereafter Halley). Thirdly, Rosetta has remained within 400 km of the nucleus for most of the mission, which is much closer than the closest approach of the flybys of other comets. Finally, Rosetta is traveling at very low velocities with respect to the comet, compared to previous mission flybys (see summary in Table 1) providing a very different perspective from which to observe plasma interaction.

One of the primary goals of the Rosetta Plasma Consortium (RPC; Carr et al. 2007) is to observe the formation and evolution of the plasma interaction regions and the boundaries between them over the time of the mission. Rosetta arrived at 67P/CG in 2014 August and the RPC suite of instruments has been making observations of the plasma environment since that time. For most of the mission Rosetta within 400 km of the nucleus in order to map the surface in great detail and to provide the best *in situ* measurements of the coma composition. In order for RPC to explore plasma boundaries close to perihelion (2015 August 13), an excursion to 1500 km distance from the comet took place during 2015 September and October. We report here the observation of the formation of two interaction regions characterized by high and low ion energies and a boundary between these regions beginning in 2015 April and lasting through 2016 January.

2 INTERACTION OF THE SOLAR WIND WITH THE COMA

2.1 Regions and boundaries

Solar wind interaction with a comet begins at great distances from the nucleus through the process of mass loading of the solar wind (e.g. Biermann et al. 1967; Galeev 1988; Johnstone 1995; Szegö et al. 2000). Boundaries represent a change in plasma parameters between one interaction region and the next. Boundaries observed by a spacecraft at a comet can be permanent features, solar wind and interplanetary magnetic field (IMF) boundaries, or small-scale transient features created by instabilities or waves (Cravens 1989). We review observations of six boundaries. Four of these boundaries, the bow shock, the cometopause, the ion pileup boundary and the contact surface, were determined to be permanent features. The 'mystery' boundary and the magnetic pileup boundary are thought to be either transient or solar wind and IMF-driven boundaries (Gringauz & Verigin 1991). The positions of the boundaries are illustrated relative to the comet in Fig. 1 (not to scale). Table 1 summarizes the distances at which boundaries were observed during four spacecraft flybys of comets Halley and 26P/GS.

Prior to spacecraft flybys of comets, computer simulations of the solar wind interaction with the comet predicted the existence of two permanent boundaries: a bow shock and a contact surface (Ip & Axford 1982; Schmidt & Wegmann 1982). Their existence was confirmed during the spacecraft flybys. Additionally, Cravens (1989) proposed the concept of various types of collisionopause, which is a permanent boundary where collisions first become important. The collisionopause location is a function of the neutral outgassing rate, the collision cross-section, the neutral outflow velocity and the ion velocity. Multiple collisionopause boundaries are possible depending on the composition of the ions and neutrals and the collision process (see Cravens 1991 for review of ion and electron collision processes).

The bow shock and the contact surface establish three general regions of comet–solar wind interaction: an upstream region outside of the bow shock, a region between the bow shock and contact surface termed the cometosheath, and a diamagnetic cavity located between the contact surface and the nucleus. Several permanent and transient features have been reported within the cometosheath: a 'mystery' boundary, the cometopause, a magnetic pileup boundary and an inner interaction region where ion densities 'pile up'.

The existence of a bow shock, a boundary where the solar wind flow transitions from supersonic to subsonic as a result of mass loading, was confirmed by several spacecraft flybys of comets (e.g. Galeev et al. 1986). Galeev et al. (1986) determined the subsolar location of the bow shock at Halley based on the combined measurements of the Vega 1 and 2 spacecraft during their respective flybys (see Table 1). The bow shock at Halley was broad, $\sim$100 000 km wide at the subsolar point and $\sim$150 000 km wide at the flank. Within such a distance, ion pickup is not negligible; hence cometary

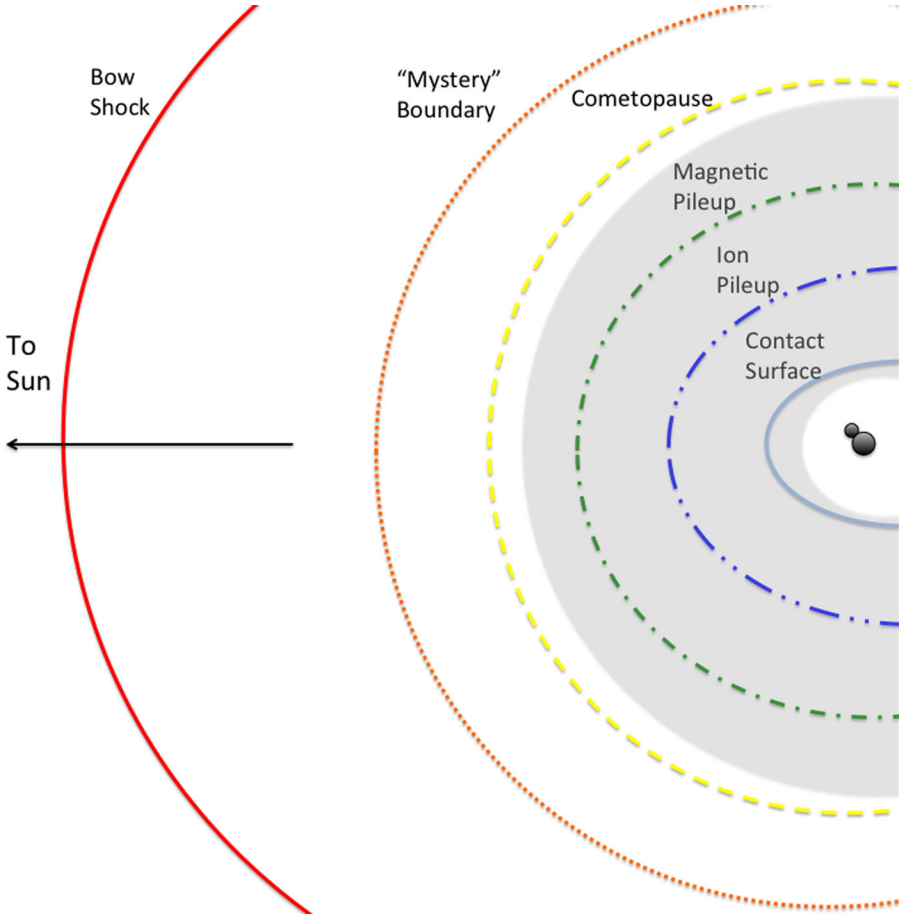

Figure 1. Illustration of the plasma interaction boundaries that have been observed during spacecraft flybys of comets. All of these boundaries, except for the mystery boundary and the magnetic pileup boundary, are thought to be permanent features of the comet–solar wind interaction. The grey shaded region is the portion of the comet solar wind interaction explored by Rosetta between 2015 May and December.

shocks are mass-loaded shocks (e.g. Mukai et al. 1986; Neubauer et al. 1990).

In the cometosheath, solar wind and cometary pickup ions are both present. During the Giotto flyby of Halley, several unexpected features were observed in the electron measurements: three outer regions and two inner regions within the cometosheath. The central outer region was named the 'mystery region' and was characterized by enhanced electron temperatures and densities that dropped suddenly when crossing a 'mystery' boundary inbound to the comet nucleus (D'Uston et al. 1988; Rème et al. 1988). Enhanced solar wind velocity and density were observed in this region as well (Fuselier et al. 1988). Theoretical models did not predict the mystery region and boundary, and their origin is not explained (Coates 1997).

The cometopause is the boundary where the ion composition in the solar wind flow changes from predominantly solar wind ions to predominantly cometary ions (Gringauz et al. 1986a; Gombosi 1987; Fuselier et al. 1988; Mendis et al. 1989; Coates 1997). Although some dispute the existence of this boundary (Rème et al. 1994), it was determined by several researchers to be a permanent feature (e.g. Gringauz & Verigin 1991; Sauer, Bogdanov & Baumgärtel 1995). Cravens (1989) defines the cometopause as the collisionopause for solar wind proton charge exchange. The location and width of the cometopause are expected to vary with time according to variations in the solar wind and the neutral gas flow parameters (Gringauz & Verigin 1991).

The region between the cometopause and the contact surface is complex and less explored by spacecraft. Inside the cometopause the dominant ions in the solar wind flow are picked-up cometary ions (Mendis et al. 1989). This is also the region where piling up of the magnetic field becomes more pronounced. Giotto observed a relatively sharp boundary at the start of the magnetic pileup region during the inbound portion of the Halley flyby and identified this as the magnetic pileup boundary (Neubauer 1988). However, a sharp boundary was not observed on the outbound leg nor on any other flyby, suggesting that an apparent sharp boundary was transient, rather than permanent feature of the comet-solar wind interaction (Gringauz & Verigin 1991).

Within the magnetic pileup region but outside of the contact surface, the Vega probes (Gringauz et al. 1986b; Vaisberg et al. 1987) and Giotto observed an ion pileup region (Balsiger et al. 1986). Inside of the ion pileup, a boundary is suggested to exist where the ion density drops by a factor of $\sim$4 and the ion density gradient changes from $1/r^2$ to $1/r$ (Coates 1997, 2009; Pätzold et al. 1997). H_3O^+ was found by Giotto to be the dominant ion species in the ion pileup region (Balsiger et al. 1986; Schwenn et al. 1988). Giotto neutral density measurements showed that ion pileup could not be explained by variations in the local spatial distribution of the neutral coma (Ip et al. 1988). This ion pileup was proposed to form because of decreasing electron recombination rates with increasing distance from the comet and increasing electron temperature with increasing distance (Ip et al. 1988; Gan & Cravens 1990; Häberli et al. 1995,

1996; Lindgren, Cravens & Ledvina 1997). Although this proposal is supported by Giotto measurements of increasing electron temperature with distance from the comet farther out from the nucleus (Eberhardt & Krankowsky 1995), the temperature of the thermal electrons relevant to the recombination rate of ions in the pileup region was not measured because of spacecraft charging effects (Häberli et al. 1996). A model that excluded dynamics showed that adjusting electron temperature could produce sufficient ion pileup to explain Giotto measurements (Häberli et al. 1996). However, plasma dynamics within the region of magnetic pileup, ion pileup and the contact surface must also be considered. Theoretical models predicted that plasma flow outside of the contact surface would be primarily stagnant with only field-aligned flow occurring (Ip et al. 1988), which was supported by Giotto ion measurements of velocities less than 0.2 km s^{-1} in the ion pileup region (Balsiger et al. 1986; Schwenn et al. 1988). Profiles of the ion velocity versus distance measured by Giotto at Halley show that the bulk ion velocity dropped from ~5 km s^{-1} to less than 1 km s^{-1} between 2.8 $\times$ 10^4 and 2.0 $\times$ 10^4 km from the nucleus, which was about 1.0 $\times$ 10^4 km before the ion pileup boundary. It is interesting to note that H_3O^+ became more abundant than H_2O^+ when velocities dropped below 1 km s^{-1} (Schwenn et al. 1988). Theoretical calculations that included both ion transport and ion loss due to electron recombination in this region showed that ion densities depend strongly on electron recombination rates when ion flow velocities are less than 1.0 km s^{-1}, but that for velocities greater than 1.0 km s^{-1} ion densities depend primarily on ion velocity (Ip et al. 1988). Furthermore, ion density enhancements were observed by Giotto to coincide with drops in the ion flow velocity (Ip et al. 1988). These observations suggest that ion pileup is not caused exclusively by changes in electron temperature and that the composition is influenced by ion flow velocity.

The existence of a region surrounding the comet nucleus that is free of any magnetic field, referred to as the diamagnetic cavity, was initially predicted by Schmidt & Wegmann (1982) and Ip & Axford (1982) and confirmed during the Giotto flyby of comet Halley (Neubauer et al. 1986). The boundary surrounding the diamagnetic cavity has been termed the ionopause (Neubauer 1988), the contact surface (Balsiger et al. 1986) or simply the diamagnetic cavity boundary (Cravens 1989). Although the diamagnetic cavity was initially proposed to be similar to the pressure ionopause at Venus, the term ionopause has since been determined to be less appropriate for comets because the cometary boundary forms mainly due to ion-neutral drage balancing magnetic pressure forces (Cravens 1986; Ip & Axford 1987). We use the term contact surface to separate the ion and magnetic effects of this boundary from the boundary that we are observing with Rosetta. Prior to the Rosetta mission, the Giotto flyby of Halley provided the only observations of the contact surface. Rosetta first observed this boundary at 67P/CG in 2015 July (Goetz et al. 2016).

2.2 The collisionopause

We determine based on a lack of observations of solar wind ions that Rosetta remained inside of the cometopause during the time period from 2015 May to December (illustrated in Fig. 1). The cometopause is suggested to be the collisionopause for charge exchange of solar wind protons. Inside of the cometopause further collisionopause boundaries could form, including an ion-neutral collisionopause that depends on the composition of the ion flow and an electron-neutral collisionopause that depends on electron energy. For this study we will look in more detail at collisionopause boundaries that could form inside of the cometopause. Comparing the boundary observations with an estimated location of the electron-neutral and ion-neutral collisionopause will provide insight into the role of collisions in forming any boundaries that RPC observes.

A collisionopause inside the cometopause would be the location where collisions between plasma and neutrals dominate the plasma dynamics as presented in Mendis et al. (1986, 1989). This boundary is similar to the exobase, which is a boundary used in aeronomy where collisions dominate the dynamic of the gas. The location of such a boundary would be where the Knudsen number, or the ratio of the mean free path to the scale height, is equal to one. The plasma mean free path, λ, is

$$\lambda = \frac{1}{n_n \sigma} \tag{1}$$

where n_n is the local neutral density and σ is the ion-neutral or electron-neutral momentum transfer cross-section. Very little information is available on momentum transfer cross-sections, which depend on the composition of the ions and neutrals, as well as the energy of the ions and electrons (Johnson et al. 2008). The electron-neutral momentum transfer cross-section has been estimated for 5 eV electrons to be ~5 $\times$ 10^{-16} cm^2 (Itikawa & Mason 2005), while the ion-neutral cross-section is estimated to be between 2 $\times$ 10^{-15} cm^2 for solar wind ions and 8 $\times$ 10^{-15} cm^2 for mass loaded solar wind with a bulk composition of H_2O^+ (Mendis et al. 1986).

According to Edberg et al. (2015) the plasma scale height at 67P observed between 2014 August and 2015 February was equal to the distance from the comet, r. Assuming that this scale height is still effective for the time period covered in this analysis, we can estimate the location of the collisionopause as the point where the distance from the comet is equal to the plasma mean free path. Since the mean free path is a function of the neutral density, we can approximate the neutral density as a function of distance from the comet as

$$n(r) = n_{s/c}\left({}^{r_{s/c}}/_{r}\right)^2 \tag{2}$$

where $n_{s/c}$ is the neutral density at the spacecraft location and $r_{s/c}$ is the distance of the spacecraft from the nucleus. Note that the neutral density measured at the spacecraft is lower than the density would be at the subsolar position (Hässig et al. 2015). We then find the location of the collisionopause by setting the mean free path equal to the distance from the comet

$$\lambda = r = n_{s/c}\sigma {r_{s/c}}^2 \tag{3}$$

The outgassing rate for 67P during 2015 ranged between 2 $\times$ 10^{26} s^{-1} and 9 $\times$ 10^{27} s^{-1} based on observations made by the Microwave Instrument for the Rosetta Orbiter (MIRO; Gulkis et al. 2007) using the method outlined in Biver et al. (2015). The neutral density at the spacecraft can be determined by the relationship

$$Q = 4\pi r^2 n_{s/c} v_n \tag{4}$$

where Q is the production rate in s^{-1}, r is the distance to the comet in meters, $n_{s/c}$ is the density at the spacecraft and v_n is the neutral velocity. The production rate can also be determined based on *in situ* neutral densities measured by the Cometary Pressure Sensor (COPS; Balsiger et al. 2007), which are not calibrated for varying gas composition. Assuming that the neutral velocity was 600 m s^{-1}, the electron-neutral collisionopause was located between 2 and 60 km of the nucleus. The ion-neutral collisionopause would be located between 8 and 955 km from the nucleus depending on the size of the cross section. Estimates for the collisionopause locations are summarized in Table 2.

Table 2. Estimated production rate and location of the electron-neutral and ion-neutral collisionopause at different time periods compared to distance of the spacecraft from the nucleus when the boundary was observed.

Time period	Production rate, Q (10^{27} s^{-1})	Source for Q	Electron-neutral collisionopause (km)	Ion-neutral collisionopause (km)	Boundary location (km)
All of 2015	0.2–9	MIRO	2–60	5–955	120–170
January to mid-April	0.2–1.2	COPS	1–8	3–130	Not observed
May to July	1.4–17	COPS	9–113	37–1800	90–300
Excursion	5.4–5.8	MIRO	35–38	143–615	540–760

3 OBSERVATIONS

3.1 The Rosetta Plasma Consortium

RPC consists of five plasma instruments designed to measure a variety of properties of the plasma environment at 67P/CG, four of which are used for this study. One of the main RPC objectives is to study the temporal evolution of the boundaries formed as a result of solar wind interaction with the coma (Carr et al. 2007). This topic includes the development, structure and dynamics of interaction regions such as the diamagnetic cavity and the region between the bow shock and the contact surface. For this study, we evaluate boundaries that form and evolve with time between the bow shock, which was not observed at any time by Rosetta, and the contact surface, which was first observed in 2015 July (Goetz et al. 2016).

The Ion and Electron Sensor (IES; Burch et al. 2007) consists of two electrostatic analyzers that measure ions and electrons with energies per charge between 4.3 eV q^{-1} to 18 keV q^{-1} with a field of view of 360° × 90°. The angular resolution is 6° × 22.°5 for the electrons and 6° × 45° for the ions.

The Ion Composition Analyzer (ICA; Nilsson et al. 2007) measures ions with energies per charge between 10 eV q^{-1} and 40 keV q^{-1} and is able to separate ions by mass with sufficient resolution to distinguish between solar wind protons and alpha particles (1 and 2 amu q^{-1}, respectively). ICA has an energy resolution (dE/E) of 7 per cent, a field of view of 360° × 90° and an angular resolution of 5° × 22.°5.

The RPC Magnetometer (MAG; Glassmeier et al. 2007b) is made up of two triaxial fluxgate magnetometers mounted on a 1.5 m boom. MAG measures the magnetic field vector with a maximum sample rate of 20 vectors per second at a resolution of 31 pT. Owing to a magnetically heavily polluted spacecraft, the uncertainty of the absolute value of the magnetic field is on the order of a few nanotesla.

Finally, the RPC Langmuir Probe (LAP; Eriksson et al. 2007) consists of two spherical Langmuir probes mounted on 2.2 m and 1.6 m booms. LAP is able to obtain spacecraft potential and ion and electron density from current measurements, depending on the influence of the spacecraft potential. In many cases since arriving at the comet, the spacecraft potential has been observed to be very negative (<-20 V). This causes low-energy electrons to be deflected away from the spacecraft, preventing LAP from providing accurate densities of electrons with energies lower than 20 eV. However, a strong negative spacecraft potential accelerates newly produced ions into IES and ICA providing an opportunity to measure ions at the earliest stages of the pickup process (Goldstein et al. 2015; Nilsson et al. 2015a,b).

In addition to the datasets from the RPC instruments, we compare observations with predictions for solar wind density, velocity and dynamic pressure at 67P/CG provided by the Michigan Solar Wind Model (mSWiM; Zieger & Hansen 2008). The mSWiM model propagates solar wind plasma measurements made near Earth to specific locations in the solar system using a 1.5-D ideal MHD model implemented with a Versatile Advection Code (Toth 1996). Unfortunately, the position of 67P/CG in relation to the Earth during the time period covered for this study does not provide optimal conditions for propagating solar wind measurements to 67P/CG, leading to uncertainties as large as 70 h in the timing of solar wind activity at 67P/CG. This uncertainty affects the analysis of events such as Corotating Interaction Regions (CIRs) or Coronal Mass Ejections (CMEs) passing the comet. It is important to note that the most accurate variable in the propagation is the solar wind velocity.

Observations in this study are divided into four time periods: (1) early 2015 January to mid-April, (2) 2015 mid-April to late July, (3) the RPC sunward excursion from 2015 late September to late October, and (4) 2015 November to 2016 February. Fig. 2 illustrates observations from IES and MAG along with mSWiM solar wind velocity predictions during the first two time periods.

3.2 2015 early January to mid-April

From 2015 January to April, 67P/CG moved from ∼2.7 to ∼1.7 au from the Sun. Neutral density measured by COPS at the location of Rosetta allows us to derive a local proxy for the water production rate using equation (4). Assuming that the neutral velocity was 600 m s^{-1}, the production rate increased from ∼2.0 × 10^{26} s^{-1} to ∼1.2 × 10^{27} s^{-1} during this time period. However, production rates determined by MIRO were much lower in mid-March ∼3.3 × 10^{26} s^{-1}. Because the coma has been found to be highly asymmetric (Hässig et al. 2015), the COPS observations identify local enhancements in the outgassing rate due to the outgassing asymmetry while the MIRO observations provide a bulk outgassing rate. Based on equation (3), the estimated location of the electron-neutral collisionopause would move from ∼1 km to ∼8 km from the nucleus during this time, assuming that the bulk electron energy is 5 eV. The location of the ion-neutral collisionopause is more difficult to estimate because of uncertainties in the ion-neutral momentum transfer cross section, which will change based on ion flow composition and energy. Depending on the size of the cross-section, it would have been located less than 3 km from the nucleus at the beginning of this time period, but could have moved out to as far as 130 km from the nucleus by 2015 mid-April.

During this time period, Rosetta was continuously orbiting 67P/CG at a distance of 30 km from the nucleus. In early 2015 February the spacecraft began to execute flybys extending up to 300 km from the comet nucleus. During one of the flybys at the end of this time period, the spacecraft experienced a navigational error where the star trackers detected too many dust grains, causing difficulties in navigation. This problem led to the data gap shown

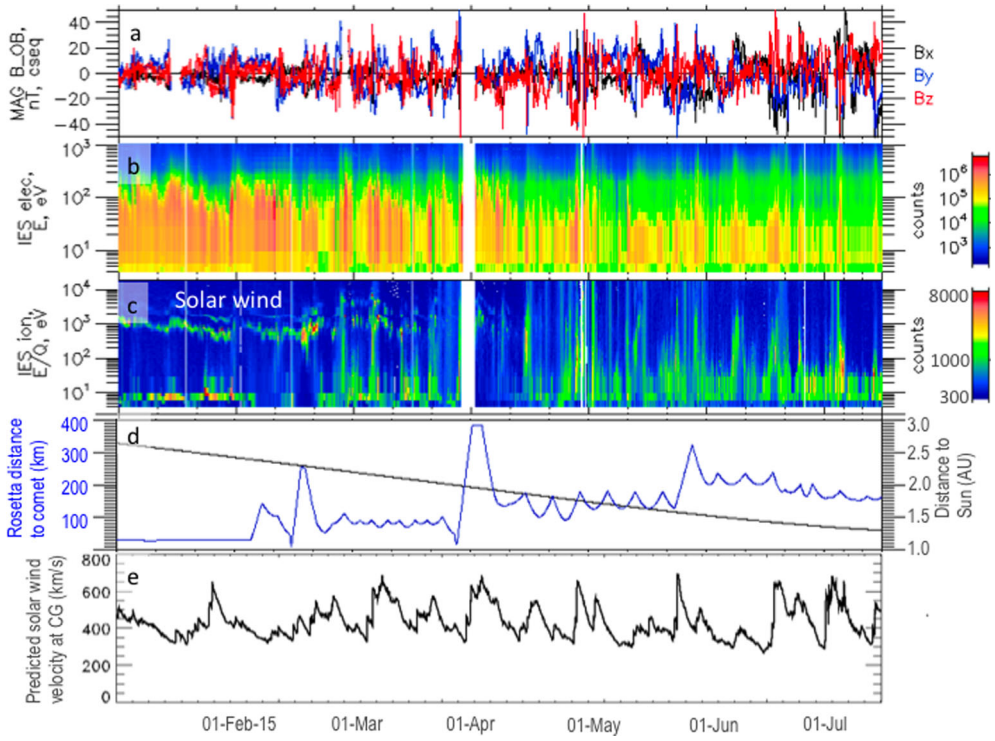

Figure 2. RPC observations from 2015 January 1 to July 31: (a) ground calibrated MAG measurements; (b) IES electron and (c) ion counts as a function of energy and time; (d) distance of Rosetta from 67P/CG (blue) and the Sun (black); and (e) mSWiM modelled solar wind velocity at 67P/CG.

in late March in Fig. 2 and forced Rosetta to operate at greater distances from the nucleus to ensure spacecraft safety. The spacecraft remained well outside of any potential electron-neutral collisionopause, but could have crossed the location of an ion-neutral collisionopause based on the calculations above.

During this time period, the IES ion spectra (illustrated in Fig. 2 panel (c) show a consistent observation of solar wind protons and alpha particles prior to 2015 April. These observations were confirmed by ICA analysis of ion composition (Nilsson et al. 2015b; Behar et al. 2016). As Fig. 2 also shows, there are time periods when the solar wind signal seems to disappear, although this disappearance is most likely due to the deflection of the solar wind outside of the IES field of view (Broiles et al. 2015; Behar et al. 2016). The variation in solar wind energy appears to increase and decrease at times similar to mSWiM predictions of changes in solar wind velocity (Fig. 2 panel e), and the peak electron energy (panel b) varies with the solar wind energy. In general, the magnetic field magnitude increases from an average value of $\sim 12 \pm 4$ nT between January 1 and 15 to $\sim 24 \pm 12$ nT between April 1 and 15, suggesting a gradual increase in magnetic pileup around the comet.

3.3 2015 mid-April to mid-July

Fig. 3 shows RPC observations during 2015 April in more detail. The regular solar wind signal disappears sometime between April 7 and 15 and is replaced by intermittent signals of ions with energies between that of the low energy ion signal and a few keV. ICA analysis of ion mass found that all of the particles observed are water group ions. We interpret the change observed to occur in mid-April to be due to the formation of a boundary between two regions and indicate with red lines times when Rosetta crossed this boundary. The inner region is characterized by low energy ions that are only observed because of acceleration of these ions into IES by the negative spacecraft potential. The low energy ions are also observed in the outer region, along with ions that are either accelerated locally or picked up far away from the nucleus, incorporated into the solar wind flow and then shocked and decelerated owing to interaction with the coma. There is also some indication of solar wind ions up to 20 April in the outer region. ICA observations of solar wind ions also end in late 2015 April (Behar et al. 2016).

The average production rate during the last half of 2015 April was 1.5×10^{27} s^{-1} with a standard deviation of 0.4×10^{27} s^{-1} according to COPS measurements. This production rate places the electron-neutral collisionopause within 12 km of the nucleus. The ion-neutral collisionopause would have been located between 30 and 200 km from the nucleus, depending on the production rate and the energy and composition of the ions. Rosetta was located between 100 and 200 km from the nucleus during the last half of April, which was well outside of the electron-neutral collisionopause but within the range of a potential ion-neutral collisionopause location.

In Fig. 3 we indicate four boundary crossings from the inner region into the outer region as identified by increases of the IES ion flux above 100 eV to values greater than $\sim$600 counts. Dashed lines indicate when Rosetta appears to have returned to the inner region based on a reduction of the IES ion flux above 100 eV. The boundary crossings do not appear to occur at a fixed distance of Rosetta from the nucleus (Fig. 3 panel d), even when taking into account the distance of Rosetta from the Sun–comet line. This observation suggests that the location of the boundary may have been shifting in response to solar wind activity.

Boundary crossing (1) is the first observed during this time period and is unique compared to the other three. At this time the solar wind signal is still clearly visible when the boundary is crossed and the accelerated water ions appear in the signal. This is an interesting time period because the interaction regions are starting to form or at least to move far enough away from the nucleus to be observed by

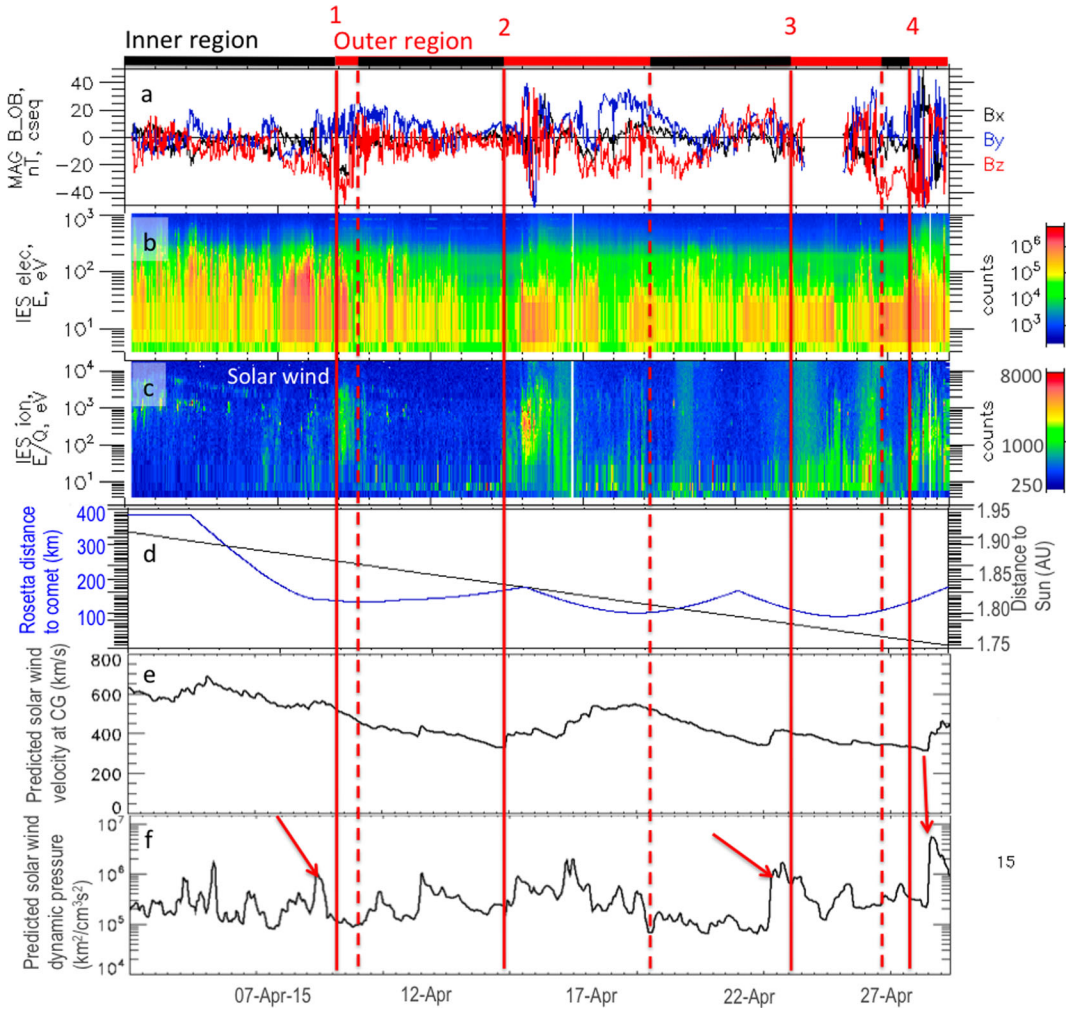

Figure 3. RPC observations for 2015 April showing plasma observations during time periods when the spacecraft is located in the inner and outer region: (a) ground calibrated MAG measurements; (b) IES electron and (c) ion counts as a function of energy and time; (d) distance of Rosetta from 67P/CG (blue) and the Sun (black); and (e) mSWiM modelled solar wind velocity and (f) dynamic pressure at 67P/CG. Four occurrences are identified with solid red lines where the IES ion spectra show ions with energies greater than 50 eV, indicating that Rosetta has crossed from an inner region to an outer region. The loss of the higher energy ions indicate that Rosetta has returned to the inner region as shown with dashed red lines. Arrows point to events discussed in text.

Rosetta. During this crossing, the distance from the spacecraft to the comet nucleus remained relatively constant. Prior to the boundary crossing, the solar wind velocity as observed by IES decreased gradually with time. The mSWiM model predicts a jump in solar wind dynamic pressure (indicated by a red arrow) less than 24 h prior to the observation of Rosetta crossing the boundary, but given the potential uncertainty of up to 70 h in the mSWiM propagation during non-optimal time periods such as those, it is possible that the increase in solar wind dynamic pressure occurred at Rosetta later than the model predicts. The length of time spent in the outer region agrees well with the length of time during which the 67P/CG coma would be exposed to elevated solar wind dynamic pressure.

Boundary crossing (2) appears to have occurred in two stages with a weak crossing that coincides almost exactly with mSWiM predictions of a solar wind velocity increase followed by a strong increase in ion energy and flux that coincides with an mSWiM prediction of a jump in solar wind dynamic pressure. Rosetta appears to have returned to the boundary with the inner region around April 16 and to remain fully within the inner region from around April 20–23. Boundary crossings (3) and (4) take place within 24 h of mSWiM predicted increases in solar wind velocity and dynamic pressure (indicated by arrows in Fig. 3). The average electron energy and flux above 100 eV increased at crossings (2) and (4).

Fig. 4 illustrates the RPC observations for the remainder of the time period in Fig. 2, while the calculated location of the collisionopause is provided in Fig. 5 (also included in Table 2). In this figure, IES does not show any signal that resembles previous solar wind signals, but there are several instances where the IES ion spectra suggest that Rosetta crossed the boundary between the inner and outer region. Also shown are the neutral densities measured by COPS (Fig. 4e). A boundary crossing into the outer region due to changes in neutral density would occur when the neutral density decreases, while returning to the inner region would result from an increase in density. Each of the boundary crossings, with the exception of (6), (8), (9) and (10), shows signs that changing neutral densities may have contributed to shifts of the boundary location.

Boundary crossings (3), (5), (6), (7), (8) and (10) take place within 24 h of a predicted sudden increase in solar wind velocity and dynamic pressure. Boundary (2) may be related to increases in solar wind velocity and dynamic pressure predicted to arrive at Rosetta around 48 h prior to the observed crossing. Boundaries (4) and

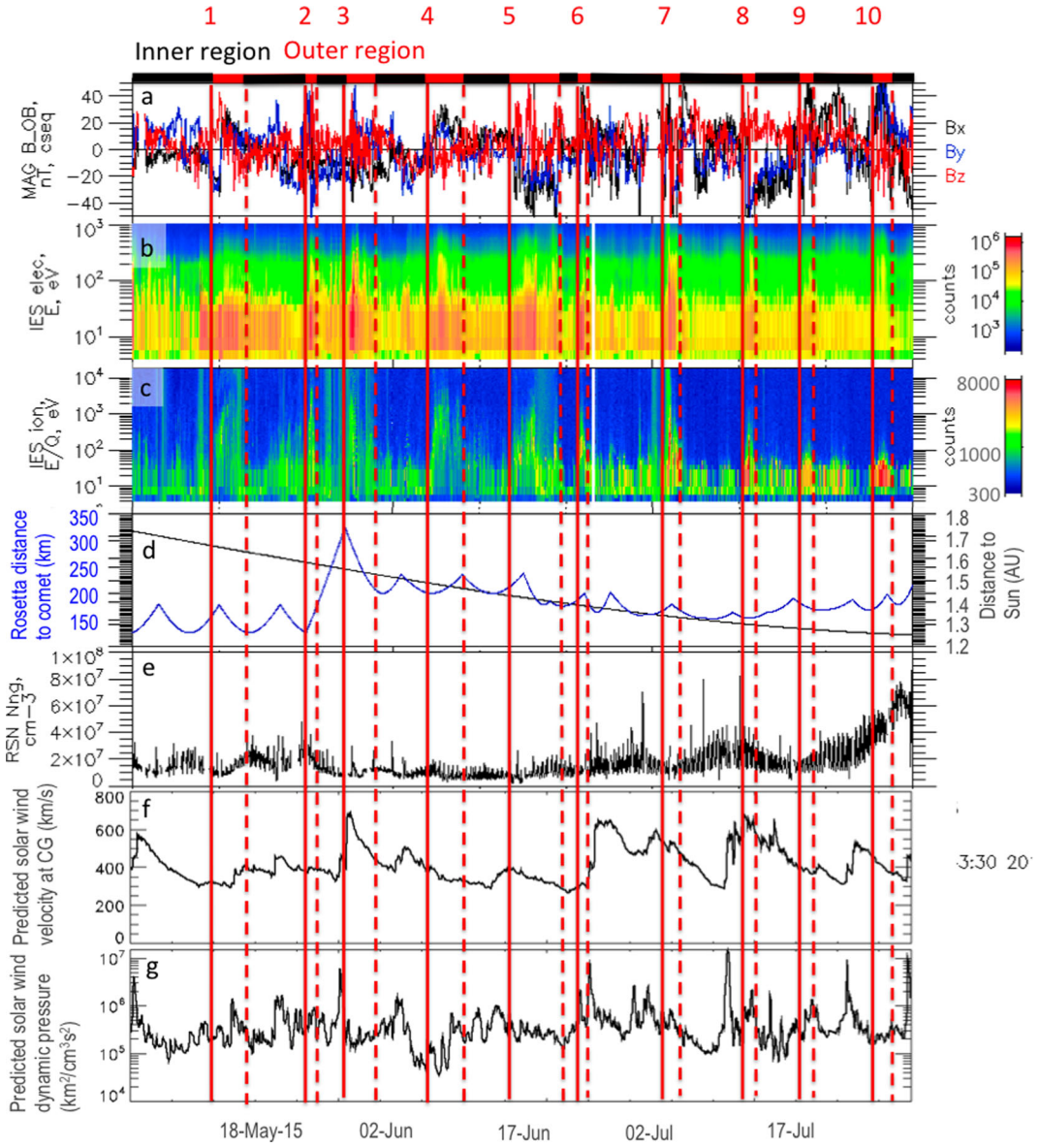

Figure 4. RPC observations for 2015 May–July: (a) ground calibrated MAG measurements; (b) IES electron and (c) ion counts as a function of energy and time; (d) distance of Rosetta from 67P/CG (blue) and the Sun (black); (e) ROSINA COPS neutral gas density at the Rosetta location; and (f) mSWiM modelled solar wind velocity and (g) dynamic pressure at 67P/CG. 10 occurrences where Rosetta appears to cross from the inner region to the outer region are indicated with solid red lines and dashed red lines indicate the approximate time when Rosetta crossed back into the inner region.

(9) coincide with brief jumps in solar wind dynamic pressure. The average electron energy and electron flux increased at all boundaries except for (1). The total magnetic field increased from an average of 32 ± 20 nT between April 15 and 30 to 40 ± 12 nT between July 15 and 30.

The apparent influence of solar wind dynamic pressure on the location of the boundary is important for understanding the nature of this boundary. As shown above, the ion-neutral collisionopause should be located within the same range of distances as that explored by Rosetta. This location depends on the momentum transfer cross section, which will decrease with increasing ion energy thus pushing the collisionopause closer to the nucleus. We illustrate in Fig. 5 the estimated location of both types of collisionopause compared to the times when RPC observed the boundary crossing between 2015 April and September. All but three of these crossings occurred within the blue shaded region where the ion-neutral collisionopause could be located. The two crossings in late July that occurred inside of the estimated ion-neutral collisionopause could have taken place at a time when increased solar wind dynamic pressure increased the ion energy and reduced the momentum-transfer cross section enough to push the boundary further inwards.

When looking closer at a few boundary crossings that occurred in a short period of time, we find that the boundary at times appears as a very sharp transition between the two regions and at other times appears broad (illustrated in Fig. 6). The boundary is likely to have been a broad transition that appears sharp as a result of dynamics of the boundary as it moves closer to and farther away from the nucleus in response to changes in solar wind dynamic pressure. In order for the boundary to appear sharp in the IES observations, it must move at a velocity equal to one width of the boundary per second.

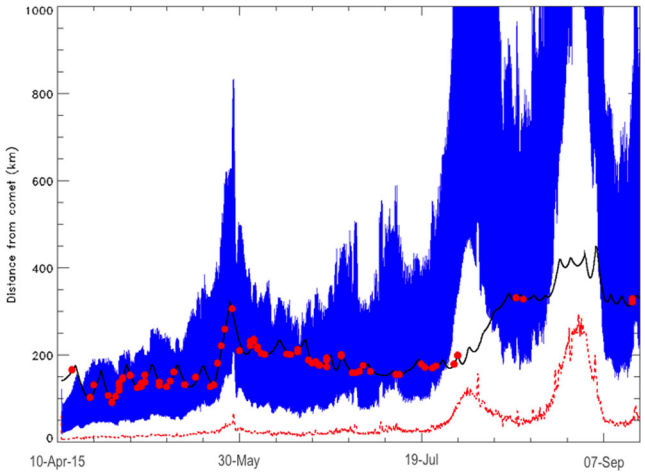

Figure 5. Comparison of the distance of Rosetta from the nucleus (black line) at the time of observed boundary crossings (red circles) with the electron-neutral (red dashed line) and ion-neutral (blue shaded region) collisionopause boundaries. Ion-neutral collisionopause estimates are based on the range of possible values for the ion-neutral momentum transfer cross-section.

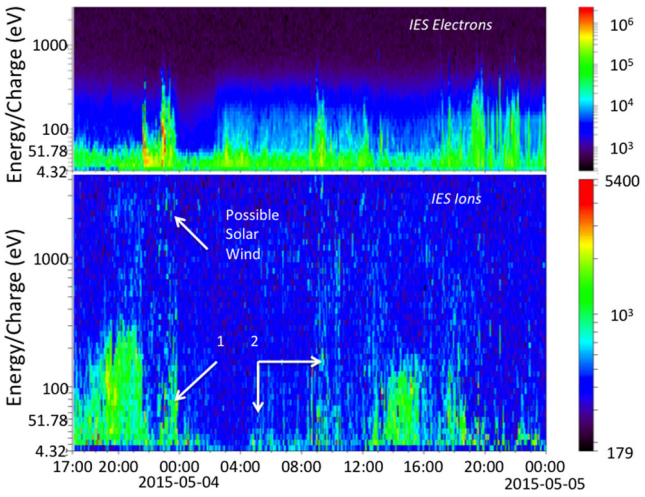

Figure 6. Illustration of sharp (1) and broad (2) boundary observations in the IES electrons (top panel) and ions (bottom panel) between 2015 03 and 04 May. The solar wind may be visible during these days. The colour bar represents counts s^{-1}.

3.4 RPC excursion and return of the solar wind

In order to explore the plasma interaction boundaries at 67P/CG, Rosetta made an excursion in 2015 September and October from normal operations within 450 km of the nucleus to a distance of 1500 km from the nucleus at a Sun–comet–spacecraft angle of ∼50°. The RPC observations for this time period are shown in Fig. 7, where the time periods in which Rosetta was within the inner and outer regions are indicated at the top of the figure. The observation of Rosetta moving into the outer region and remaining in the outer region for several days until returning to a position closer to the comet (∼600 km) confirms that the boundary is a permanent feature of the solar wind-comet interaction at 67P/CG.

Although Rosetta moved well into the outer region during the excursion, there is no obvious solar wind proton or alpha signal around 1 keV like was observed before early May. In early October there is a possible solar wind He^{++} signal at energies ∼2 keV in the time period leading up to a CME that passed Rosetta and 67P/CG on October 6. At the time of this writing, mSWiM solar wind simulations were not available for the excursion time period.

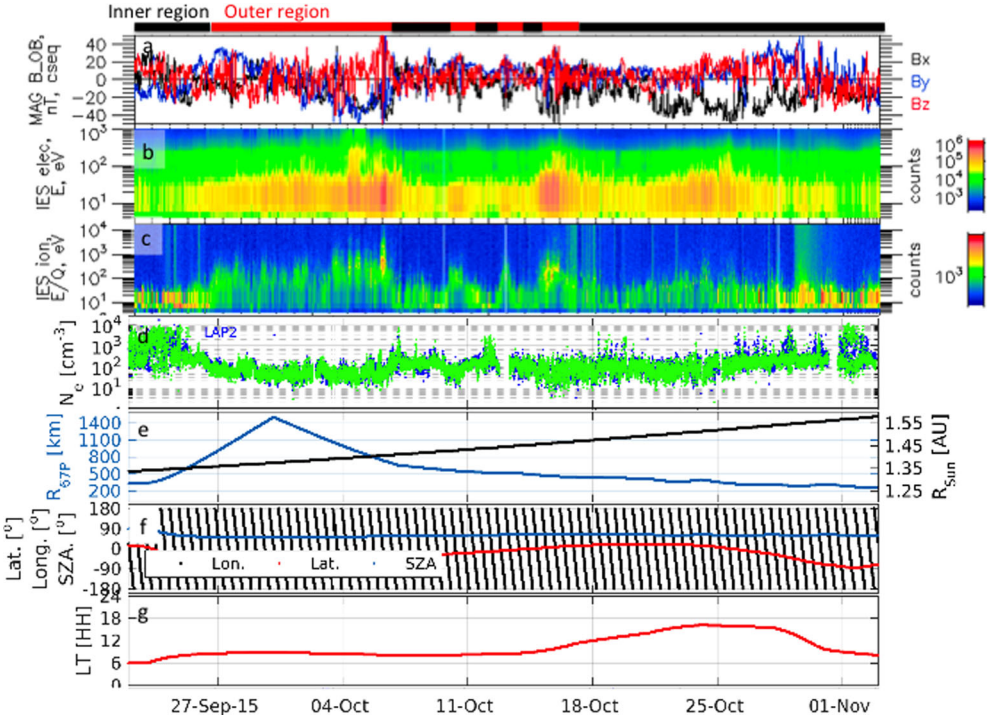

Figure 7. RPC observations during the excursion: (a) ground calibrated MAG measurements; (b) IES ion and (c) electron counts as a function of energy and time; (d) LAP electron density; (e) distance of Rosetta from 67P/CG (blue) and the Sun (black); (f) solar zenith angle and the longitude and latitude below the spacecraft; and (g) Local time at the location of the comet below the spacecraft.

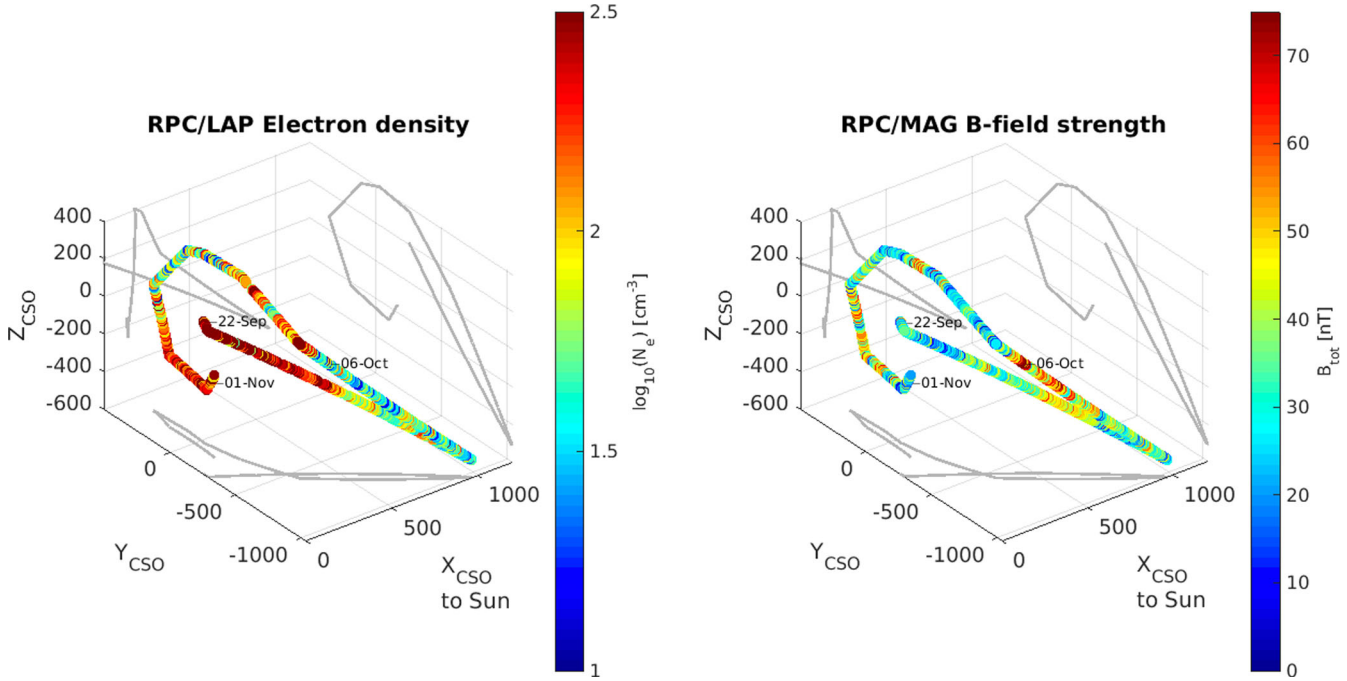

Figure 8. RPC observations of electron density (left) and magnetic field magnitude (right) during the excursion in the body-Centred Solar Orbital (CSO) coordinates with distances given in km. In the CSO reference frame, the nucleus is at the origin, the Sun is in the minus-x direction, the y-axis is orthogonal to the x-axis in the direction of the motion of the comet around the Sun and the z-axis completes the right-handed reference frame.

The electron density was high and the spacecraft potential (not shown) was strongly negative (<-5 V) in the inner region while the spacecraft potential became positive and the electron densities decreased within the outer region. IES electron observations show an enhanced suprathermal electron flux (energies greater than 100 eV) in the outer region. As illustrated in Fig. 8, the magnetic field magnitude was greater in the outer region than in the inner region. Fig. 8 also shows that the electron density was higher in the inner region compared to the outer region.

Observations of the boundary continued until an intermittent solar wind signal reappeared in 2016 mid-January. At this time the comet moved beyond 2.0 au from the Sun.

3.5 Characteristics of the regions and boundary

The RPC excursion was the most informative time period for evaluating the plasma characteristics of the two regions observed. In Fig. 9 we illustrate how the calibrated magnetic field magnitude, the electron density determined by LAP and the ion velocity moment derived from the IES ion observations change as a function of distance from the comet during the excursion. The magnetic field and electron density measurements were binned and interpolated to the lower time resolution of the IES measurements to allow correlation of the resampled parameters. Boundary crossings were observed at distances between 575 and 760 km from the nucleus during the time covered in the figure. In Fig. 9 the ion velocities and the magnetic field appeared to increase and decrease together, while the electron density showed a very weak trend of decreasing when the magnetic field and ion velocity increased. To quantify this apparent relationship we calculated the Pearson correlation coefficient for several plasma parameters. This correlation study allows us to determine if there is a clear difference between the plasma conditions in the inner region compared to the outer region.

In Table 3 we give the correlation coefficients for the full resolution (black circles in Fig. 9) IES ion density, temperature and velocity, and the resampled LAP electron density and the MAG calibrated magnetic field magnitude. Electron temperature measurements are not available at this time owing to large uncertainties in deriving this property from the LAP measurements. However, we compare with the spacecraft potential, which is a function of both the electron density and temperature and is measured with greater accuracy by LAP.

The Pearson correlation coefficient shows that all parameters have positive correlation coefficients with the exception of the magnetic field magnitude and the electron density. This result agrees with the observations shown in Fig. 9 where the electron density increases slightly when the magnetic field decreases. Significant correlation only occurs between the magnetic field magnitude and the ion temperature and velocity.

Based on this comparison of datasets, we find that the ions in the inner region have lower flow velocities and lower temperatures, that the electron densities are higher and that the magnetic field magnitude is reduced. Ions in the outer region have velocities greater than 5 km s^{-1} and higher temperatures, while electron densities are lower and the magnetic field magnitude is increased. Therefore, the ion velocity and temperature, the electron density and the magnetic field magnitude all change across the boundary.

3.6 Boundary location

As explained before, the location of the boundary between the two regions appears to vary both with the cometary neutral gas production rate and with the solar wind dynamic pressure. The uncertainty is large in the predicted solar wind dynamic pressure at 67P/CG based on measurements made near the Earth. This uncertainty makes numerical comparison with the measured boundary locations difficult. However, the production rate of cometary gas is

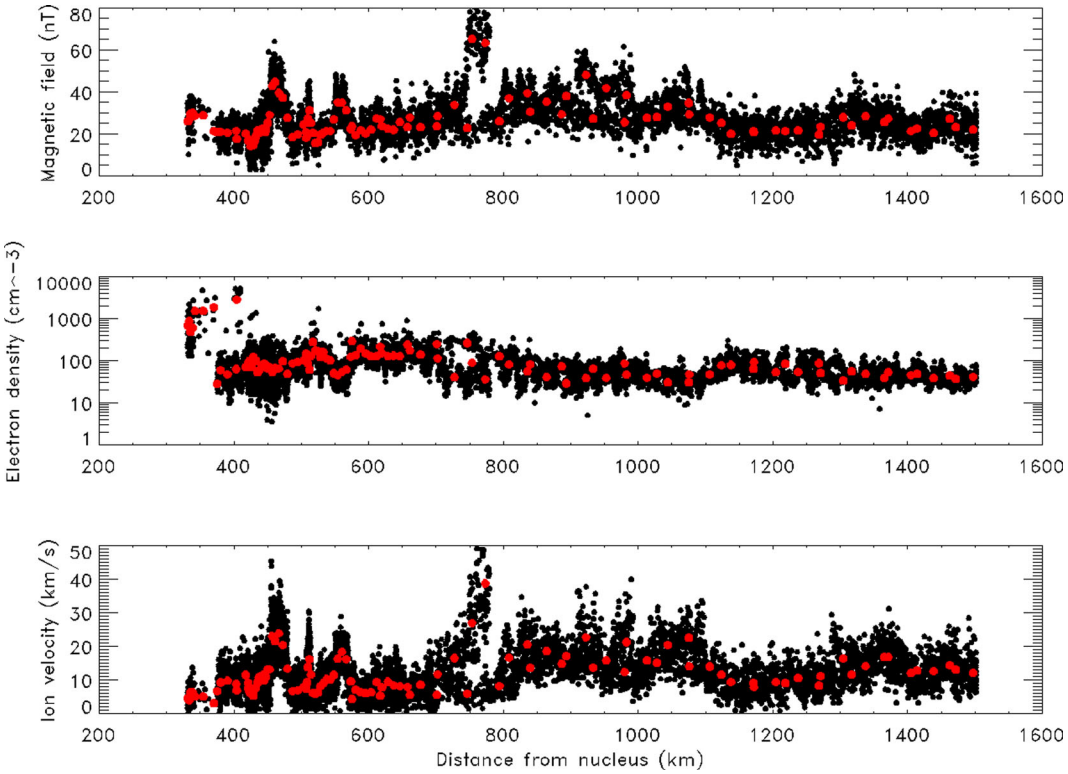

Figure 9. Derived plasma parameters (black circles) as a function of distance from the comet during the RPC excursion. Measurements are binned into averages over 15 min (red circles).

Table 3. Correlation study results for the derived plasma parameters measured during the RPC excursion.

Parameters		Pearson correlation coefficient
IES Ion density (n_i)	LAP Electron density (n_e)	0.49
IES log(n_i)	LAP log(n_e)	0.68
MAG Magnetic field magnitude (B)	LAP log(n_e)	–0.32
MAG B	IES log(n_i)	0.10
MAG B	IES Ion velocity (v_i)	0.88
MAG B	IES Ion temperature (T_i)	0.72
MAG B	LAP Spacecraft potential	0.35

estimated by the *in situ* measurement of the neutral density made by the ROSINA COPS instrument and the MIRO full coma observations. We now attempt to see if the location of the boundary can be predicted by fitting the observations to the production rates.

We illustrate in Fig. 10 the location of the boundary along the Sun–comet line, assuming that the shape of the boundary is a parabola. The distance of the boundary from the nucleus appears to have increased linearly with the derived production rate in agreement with previous studies of boundary locations (e.g. Galeev et al. 1986; Gringauz & Verigin 1991), but with a large degree of scattering around the line. However, we note that our observations for the location of this boundary are limited to the distances explored by the Rosetta spacecraft, so observations beyond 450 km from the nucleus are restricted to the time period of the excursion. The Pearson correlation coefficient and the linear fit parameters for these observations are provided in Table 4.

In each case the correlation is relatively strong, but the slope and intercept vary significantly between comparisons. The intercept in

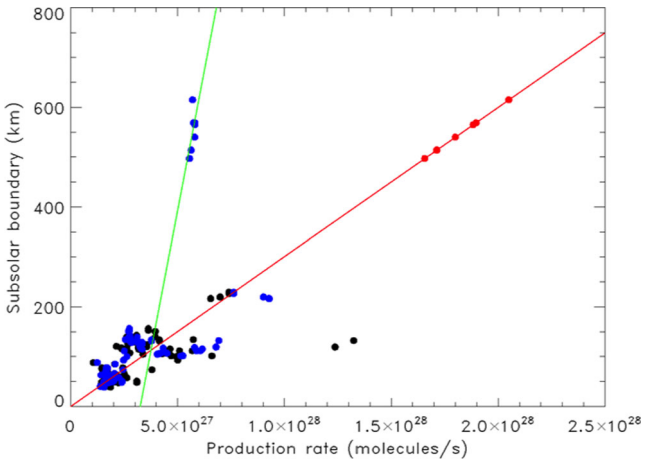

Figure 10. Estimated distance of the boundary from the nucleus of 67P/CG along the Sun–comet line assuming a parabolic shape for the boundary compared to production rates derived from COPS (black circles) and MIRO (blue circles). The red line represents a linear fit of the boundary location to the COPS production rate assuming an intercept of zero. The COPS production rates during the excursion are predicted by the linear fit based on the location of the boundary crossings along the Sun–comet line (red circles). The green line is the linear fit to MIRO production and boundary locations observed during the excursion. Unfortunately, COPS was not operating during the excursion, so local production rates are not available for these boundary observations.

the linear fits could theoretically be used to determine a minimum production rate for the boundary to form. However, the negative intercept in the cases including data prior to the excursion requires that the boundary exist without any production, while the large

Table 4. Correlation coefficients and linear fit parameters for the boundary location compared to measurements of the production rate.

Production source	Pearson correlation	x-Intercept	Slope	y-Intercept
COPS	0.68	56	1.4e-26	-4.0×10^{27}
MIRO excluding excursion	0.78	41	1.9e-26	-2.2×10^{27}
MIRO all observations	0.58	10	3.6e-26	-2.7×10^{26}
MIRO excursion only	0.56	−730	2.2e-25	3.3×10^{27}

intercept for the excursion production rate fits is greater than the measured production rate during more than half of the boundary crossings as illustrated in Fig. 10 (green line).

Since the minimum production rate must be greater than zero, we fit a line to the COPS production rate fixing the intercept at zero

$$R_B = (3.0 \pm 0.5) \times 10^{-26} Q \quad (5)$$

where R_B is the distance in km of the boundary from the nucleus along the Sun–comet line. This gives a model for estimating the COPS production rate that would have been measured during the excursion had COPS been operating, based on the observed location of the boundary. We then compare this estimated production rate with the production rate observed by MIRO. As Fig. 10 illustrates, this fit predicts a significantly higher production rate during the excursion than MIRO measured.

Therefore, we conclude that it is not possible to constrain the location of the boundary based on the production rate alone as demonstrated by how the predicted production rate during the excursion was much greater than that measured by MIRO. Furthermore, this result demonstrates the importance of solar wind velocity and density in determining the location of the boundary. Given the large uncertainty in the model predictions for solar wind parameters, we are not able to derive an equation to represent the boundary location at this time and leave it to future work that includes modelling.

4 DISCUSSION

RPC observations show that solar wind–cometary plasma interaction boundaries and regions formed in the time period between 2015 mid-April and mid-May when 67P/CG was ∼1.8 au from the Sun and the COPS-derived production rate of the comet was $\sim 1.2 \times 10^{27}$ s^{-1}. After mid-April RPC observed at least two regions that are separated by a broad boundary that appears to move inwards and outwards in response to changes in local neutral density and in solar wind dynamic pressure. All but three of the observed boundary crossings occurred within the region where an ion-neutral collisionopause could form. Although the boundary appears to be sharp in some cases, as illustrated in Fig. 6, the sharp appearance is most likely due to the motion of the boundary relative to the spacecraft as a result of changes in solar wind dynamic pressure.

The inner region is characterized by low energy ions that appear in the IES ion energy spectra near the value of the spacecraft potential as measured by LAP (e.g. $E_i = 5$ eV when $\phi = -5$ V), while the outer region is characterized by relatively high energy ions observed in the IES ion spectra confirmed by ICA to be water-group ions (Nilsson et al. 2015a,b; Behar et al. 2016). Comparison of observations made during the excursion show that LAP electron densities in the inner region are enhanced while the magnetic field magnitude is reduced compared to the outer region. The electron flux above 100 eV is reduced within the inner region suggesting a reduction in suprathermal electrons. The boundary between the inner and outer regions was located well outside of the diamagnetic cavity (Goetz et al. 2016). This boundary is not predicted by model simulations intended to evaluate the plasma interaction at 67P/CG (e.g. Koenders et al. 2015). However, it bears a strong resemblance to the drop in ion velocity observed by Giotto at the start of the ion pileup region at Halley (Schwenn et al. 1988). The strong correlation between the magnetic field magnitude and the ion temperature and velocity moments suggests that the ion flow and the magnetic field are strongly coupled. Enhanced electron densities inside the boundary resemble the ion pileup region observed at Halley.

The solar wind signal disappeared between 2016 early May 2015 and mid-January, and was only observed during the excursion well outside the boundary just prior to the impact of a CME at 67P/CG. This suggests that Rosetta remained well within the boundary where cometary ions become the dominant ion species, or the cometopause, during the entire time period. One thing that must be noted, however, is that the deflection of the mass-loaded solar wind flow was observed to be mass dependent (Broiles et al. 2015). It is possible that the solar wind protons and alpha particles are deflected away from the nucleus beyond the region where Rosetta was located while the heavier picked up cometary ions continued flow inwards towards the nucleus. Depending on the ion-neutral collision rate, it is even possible for the picked up ions to form a collisionopause, or a boundary where the flow stagnates because of collisions. However, local acceleration of ions by the solar wind electric field cannot be ruled out by the observations.

The location of the boundary observed by Rosetta along the Sun–comet line appears to vary linearly with the production rate, but observations are biased to a small region of sampling space. Furthermore, attempts to model the boundary location as a function of production rate do not predict the production rate observed by MIRO during the excursion. This suggests that production rate alone cannot predict the boundary location and that solar wind dynamic pressure plays an important role in its position.

Comparisons of the boundary location with the ion-neutral collisionopause estimates show that most boundary observations were within the predicted region of this collisionopause. This result suggests that collisions play an important role in the slowing of the ion flow that is the main characteristic of the observed boundary.

5 CONCLUSIONS

RPC has observed two regions separated by a broad boundary. The excursion confirmed that this boundary is a permanent feature of the solar wind interaction. As illustrated in Figs 7, 8 and 10, during the RPC excursion Rosetta moved across the boundary from an inner region to an outer region and remained in the outer region for a long time period, only returning to the inner region when returning to a distance similar to the earlier crossing of the boundary. The ion temperature and velocity are strongly correlated with the magnetic field magnitude and the electron density is weakly correlated with the magnetic field. The location of the boundary appears to be within the region where collisions between ions and neutrals become important and appears to be strongly influenced by the solar wind dynamic pressure.

ACKNOWLEDGEMENTS

Rosetta is an ESA mission with contributions from its Member States and the U.S. National Aeronautics and Space Administration

(NASA). The work on IES and ROSINA were supported by NASA through contracts no. 1345493 and 1496541 with the Jet Propulsion Laboratory, California Institute of Technology. Support for RPC-MAG is provided by the German Ministerium für Wirtschaft und Energie and the Deutsches Zentrum für Luft- und Raumfahrt under contract 50QP 1401. Work at the University of Bern on ROSINA/COPS was funded by the State of Bern, the Swiss National Science Foundation, and the European Space Agency PRODEX Programme. CSW is supported by the Research Council of Norway grant no. 240000. We thank the teams at Imperial College London and ESA who have been responsible for the operation of IES. We acknowledge the staff of CDPP and IC for the use of AMDA and the RPC Quicklook database (provided by a collaboration between the Centre de Données de la Physique des Plasmas, supported by CNRS, CNES, Observatoire de Paris and Université Paul Sabatier, Toulouse and Imperial College London, supported by the UK Space Agency). Finally, we thank Tom Cravens for his helpful review of this manuscript.

REFERENCES

Balsiger H. et al., 1986, Nature, 321, 330
Balsiger H. et al., 2007, Space Sci. Rev., 128, 745
Behar E., Nilsson H., Wieser G. S., Nemeth Z., Broiles T. W., Richter I., 2016, Geophys. Res. Lett., 43, 1411
Biermann L., Brosowski B., Schmidt H. U., 1967, Solar Phys., 1, 254
Biver N. et al., 2015, A&A, 583, A3
Broiles T. W. et al., 2015, A&A, 583, A21
Burch J. L. et al., 2007, Space Sci. Rev., 128, 697
Carr C. et al., 2007, Space Sci. Rev., 128, 629
Coates A. J., 1997, Adv. Space Res., 20, 255
Coates A. J., 2009, in Ao X., Burrows R. H., Zank G. P., eds, 18th Annu. Int. Astrophys. Conf. Vol. 1183, Shock Waves in Space and Astrophysical Environments. AIP Publishing, Melville, NY, p. 121
Coates A. J., Johnstone A. D., Neubauer F. M., 1996, J. Geophys. Res.: Space Phys., 101, 27573
Cravens T. E., 1986, in Battrick B., Rolfe E. J., Reinhard R., eds, Proc. 20th ESLAB Symp. SP-250, Exploration of Halley's Comet. Eur. Space Agency Spec. Publ., Noordwijk, the Netherlands, p. 244
Cravens T. E., 1989, Adv. Space Res., 9, 293
Cravens T. E., 1991, in Johnstone A., ed., Collisional Processes in Cometary Plasmas, in Cometary Plasma Processes. American Geophysical Union, Washington, p. 27
d'Uston C. et al., 1988, in Grewing M., Praderie F., Reinhard R., eds, Exploration of Halley's Comet. Springer, Berlin, p. 137
Eberhardt P., Krankowsky D., 1995, A&A, 295, 795
Edberg N. J. et al., 2015, Geophys. Res. Lett., 42, 4263
Eriksson A. I. et al., 2007, Space Sci. Rev., 128, 729
Fuselier S. A. et al., 1988, Geophys. Res. Lett., 15, 549
Galeev A. A., 1988, in Grewing M., Praderie F., Reinhard R., eds, Exploration of Halley's Comet. Springer, Berlin, p. 12
Galeev A. A. et al., 1986, Geophys. Res. Lett., 13, 841
Gan L., Cravens T. E., 1990, J. Geophys. Res., 95, 6285
Glassmeier K. H., Boehnhardt H., Koschny D., Kührt E., Richter I., 2007a, Space Sci. Rev., 128, 1
Glassmeier K. H. et al., 2007b, Space Sci. Rev., 128, 649
Goetz C. et al., 2016, A&A, 588, A24
Goldstein R. et al., 2015, Geophys. Res. Lett., 42, 3093
Gombosi T. I., 1987, Geophys. Res. Lett., 14, 1174
Gringauz K. I. et al., 1986a, Geophys. Res. Lett., 13, 613
Gringauz K. I., Verigin M. I., Richter A. K., Gombosi T. I., Szegö K., Tatrallyay M., Remizov A. P., Apathy I., 1986b, in Grewing M., Praderie F., Reinhard R., eds, ESLAB Symp. Vol. 250, Exploration of Halley's Comet. Springer, Berlin, p. 93
Gringauz K. I., Verigin M. I., 1991, in Johnstone A., ed., Permanent and Nonstationary Plasma Phenomena in Comet Halley's Head, in Cometary Plasma Processes. American Geophysical Union, Washington, p. 107
Gulkis S. et al., 2007, Space Sci. Rev., 128, 561
Häberli R. M., Altwegg K., Balsiger H., Geiss J., 1995, A&A, 297, 881
Häberli R. M., Altwegg K., Balsiger H., Geiss J., 1996, J. Geophys. Res.: Space Phys., 101, 15579
Hässig M. et al., 2015, Science, 347, aaa0276
Ip W. H., Axford W. I., 1982, in Wilkening L. L., ed., Proc. IAU Colloq. 61, Vol. 1, Comet Discoveries, Statistics, and Observational Selection. Univ. Arizona Press, Tucson, AZ, p. 588
Ip W.-H., Axford W. I., 1987, Nature, 325, 418
Ip W. H., Schwenn R., Rosenbauer H., Balsiger H., Neugebauer M., Shelley E. G., 1988, in Grewing M., Praderie F., Reinhard R., eds, Exploration of Halley's Comet. Springer, Berlin, p. 132
Itikawa Y., Mason N., 2005, Phys. Chem. Ref. Data, 34, 1
Johnson R. E. et al., 2008, Space Sci. Rev., 139, 355
Johnstone A. D., 1995, Adv. Space Res., 16, 11
Johnstone A. D. et al., 1993, A&A, 273, L1
Koenders C., Glassmeier K. H., Richter I., Ranocha H., Motschmann U., 2015, Planet. Space Sci., 105, 101
Lindgren C. J., Cravens T. E., Ledvina S. A., 1997, J. Geophys. Res.: Space Phys., 102, 17395
Mendis D. A., Smith E. J., Tsurutani B. T., Slavin J. A., Jones D. E., Siscoe G. L., 1986, Comet Encounters, 13, 239
Mendis D. A., Flammer K. R., Reme H., Sauvaud J. A., D'Uston C., 1989, Ann. Geophys., 7, 99
Mukai T. et al., 1986, Geophys. Res. Lett., 13, 829
Neubauer F. M., 1988, in Grewing M., Praderie F., Reinhard R., eds, Exploration of Halley's Comet. Springer, Berlin, Heidelberg, p. 73
Neubauer F. M. et al., 1986, Nature, 321, 352
Neubauer F. M., Glassmeier K. H., Acuna M. H., Mariani F., Musmann G., 1990, Ann. Geophys., 8, 463
Neubauer F. M. et al., 1993, A&A, 268, L5
Nilsson H. et al., 2007, Space Sci. Rev., 128, 671
Nilsson H. et al., 2015a, Science, 347, aaa0571
Nilsson H. et al., 2015b, A&A, 583, A20
Pätzold M., Neubauer F. M., Andreev V. E., Gavrik A. L., 1997, J. Geophys. Res.: Space Phys., 102, 2213
Rème H. et al., 1988, in Grewing M., Praderie F., Reinhard R., eds, Exploration of Halley's Comet. Springer, Berlin, p. 33
Rème H., Mazelle C., d'Uston C., Korth A., Lin R. P., Chaizy P., 1994, J. Geophys. Res., 99, 2301
Sauer K., Bogdanov A., Baumgärtel K., 1995, Adv. Space Res., 16, 153
Schmidt H. U., Wegmann R., 1982, in Vilkening L. L., ed., Comet: Gases, Ices, Grains and Plasma. Univ. Arizona Press, Tuscon, AZ, p. 538
Schwenn R., Ip W. H., Rosenbauer H., Balsiger H., Bühler F., Goldstein R., Shelley E. G., 1988, in Grewing M., Praderie F., Reinhard R., eds, Exploration of Halley's Comet. Springer, Berlin, p. 160
Szegö K. et al., 2000, Space Sci. Rev., 94, 429
Toth G., 1996, Astrophys. Lett. Commun., 34, 245
Vaisberg O. L., Smirnov V. N., Gorn L. S., Iovlev M. V., 1987, Cosm. Res., 25, 867
Zieger B., Hansen K. C., 2008, J. Geophys. Res.: Space Phys., 113, A08107

[1]*Space Science and Engineering Division, Southwest Research Institute, 6220 Culebra Rd, San Antonio, TX 78228, USA*
[2]*Department of Physics and Astronomy, University of Texas at San Antonio, San Antonio, TX 78249, USA*
[3]*IRF Swedish Institute of Space Physics Uppsala, SE-75121 Uppsala, Sweden*
[4]*Technical University of Braunschweig, D-38106 Braunschweig, Germany*
[5]*Laboratoire de Physique et Chimie de l'Environnement et de l'Espace, F-45071 Orléans Cedex 2, France*
[6]*Wigner Research Centre for Physics, H-1121 Budapest, Hungary*
[7] *Department of Radio Science and Engineering, Aalto University, RADELEC, FI-00076 Aalto, Finland*

[8] *Laboratiore d'Études Spatiales et d'Instrumentation en Astrophysique, Observatoire de Paris, Section de Meudon, 5 place Jules Janssen, F-92196 Meudon Cedex, France*
[9] *Imperial College London, London SW7 2AZ, UK*
[10] *Mullard Space Science Laboratory, University College of London, London RH5 6NT, England*
[11] *University of Michigan, Ann Arbor, MI 48109, USA*
[12] *IRF Swedish Institute of Space Physics Kiruna, SE-981 28 Kiruna, Sweden*
[13] *NASA/GSFC, Greenbelt, MD 20771, USA*
[14] *Physikalisches Institut, University of Bern, CH-3012 Bern, Switzerland*
[15] *Space Research Institute, Austrian Academy of Sciences, A-8042 Graz, Austria*
[16] *Department of Physics, University of Oslo, P.O. Box 1048 Blindern, N-0316 Oslo, Norway*

This paper has been typeset from a TEX/LATEX file prepared by the author.